LUND UNIVERSITY

Six DOF Eye-to-Hand Calibration from 2D Measurements Using Planar Constraints

Bagge Carlson, Fredrik; Johansson, Rolf; Robertsson, Anders

Six DOF Eye-to-Hand Calibration from 2D Measurements Using Planar Constraints

Fredrik Bagge Carlson*   Rolf Johansson   Anders Robertsson

Abstract— **This article presents a linear, iterative method to solve the eye-to-hand calibration problem between a wrist-mounted laser scanner and the tool flange of a robot. Measurement data are acquired from a set of non parallel planes whereafter the plane equations and desired rigid transformation matrix are found in a two-step, iterative fashion. The method is shown to handle large error in the initial estimate of the transform and results are verified in both simulations and experiments using a seam tracking laser sensor for welding applications.**

Index Terms— **calibration, laser scanner, eye to hand, eye in hand, kinematic calibration**

I. INTRODUCTION

Laser scanners have been widely used for many years in the field of robotics. A large group of laser scanners, such as 2D laser range finders and laser stripe profilers, provide accurate distance measurements confined to a plane. By moving either the scanner or the scanned object, a 2D laser scanner can be used to build a 3D representation of an object or the environment. To this purpose, laser scanners are commonly mounted on mobile platforms or robots.

This work considers the calibration of a wrist mounted laser scanner for robotic 3D scanning and weld seam tracking applications. To relate the measurements of the scanner to the robot coordinate system, the rigid transformation between the scanner coordinate system and the tool flange of the robot is needed.

A naive approach to the stated calibration problem is to make use of the 4/5/6-point tool calibration routines commonly found in industrial robot systems. These methods suffer from the fact that the origin and the axes of the sensor coordinate system are invisible to the operator, which must rely on visual feedback from both the workspace and a computer monitor simultaneously. Further, the accuracy of these methods is very much dependent on the skill of the operator and data collection for even a small amount of points is very tedious.

Other well known algorithms for eye-to-hand calibration include [1], [2], [3], which are all adopted for
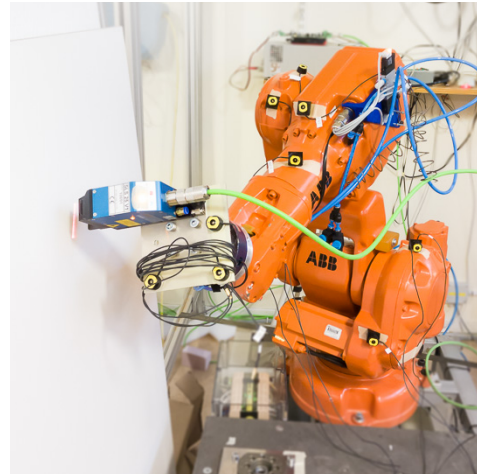
Fig. 1.   ABB IRB140 used for experimental verification.

calibration of a wrist-mounted camera using a calibration pattern. A laser scanner is fundamentally different in the information it captures, which must be considered by the calibration algorithm employed.

Kinematic calibration of robotic manipulator using planar constraints in various formats has been considered before. In [4], the proposed method begins with an initial estimate of the desired parameters, which is improved with a non-linear optimization algorithm. The authors also discuss observability issues related to identification using planar constraints. The method focuses on improving parameter estimates in the kinematic model of the robot, and convergence results are therefore only presented for initial guesses very close to their true values $(0.01\text{mm}/0.01°)$.

In [5], the transformation between a camera and a laser range finder is found using a checker board pattern and computer vision to estimate the location of the calibration planes. With the equations of the calibration planes known, the desired transformation matrix is obtained from a set of linear equations.

Planar constraints have also been considered in [6] where the authors employ a non-linear optimization technique to estimate the kinematic parameters. The method requires careful definition of the planes and can not handle arbitrary frame assignments.

A wrist mounted sensor can be seen as an extension of the kinematic chain of the robot. Initial guesses can be poor, especially if based on visual estimates. This paper presents a method based solely on solving linear

sets of equations. The method accepts a very crude initial estimate of the desired kinematic parameters, which is refined in an iterative procedure. The placement of the calibration planes is assumed unknown, and their locations are found together with the desired transformation matrix.

The article is structured as follows, preliminary equations and notation are covered in Sec. II followed by the introduction of the proposed approach in Sec. III. Section IV presents a simulation study of convergence properties as well as experimental verification of the approach. Conclusions are finally given in Sec. V.

II. Preliminaries

Throughout the paper the following notation will be used. A subscript denotes the frame of reference, such that the coordinates of a point p_A are given in the frame A. $T_A^B \in SE(4)$ denotes a transformation matrix from frame A to frame B such that [7]

$$T_A^B \mathbf{p}_B = \mathbf{p}_A \tag{1}$$

The matrix T_A^B can be decomposed into R_A^B and p_A^B such that

$$T_A^B = \begin{bmatrix} R_A^B & p_A^B \\ \mathbf{0} & 1 \end{bmatrix} \tag{2}$$

The normal of a plane from which measurement point i is taken, given in frame A, will be denoted n_A^i.

A plane is completely specified by

$$n^\mathsf{T} p = d, \quad \|n\|_2 = 1 \tag{3}$$

where d is the orthogonal distance from the origin to the plane, n the plane normal and p is any point on the plane.

A. Laser scanner characteristics

The laser scanner consists of a camera and a laser source emitting light in a plane which intersects a physical plane in a line. The three dimensional location of a point along the projected laser line may be calculated by triangulation, based on a known geometry between the camera and the laser emitter. A single measurement from the laser scanner typically yields the coordinates of a large number of points in the laser plane, alternatively, a measurement consists of a single point and the angle of the surface, which is easily converted to two points.

III. METHOD

The objective of the calibration is to find the transformation matrix $T_{TF}^S \in SE(4)$ that relates the measurements of the laser scanner to the coordinate frame of the tool flange of the robot.

The kinematic chain of a robot manipulator will here consist of the transformation from the robot base frame to the tool flange $T_{RB}^{TF_i}$, given by the manipulator forward kinematics in pose i, and the transformation from the tool flange to the sensor T_{TF}^S. The sensor, in turn, projects laser light onto a plane with unknown equation. A point
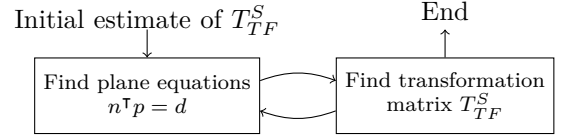

Fig. 2. Illustration of the two-step, iterative method.

observed by the sensor can be translated to the robot base frame by

$$\mathbf{p}_{RB_i} = T_{RB}^{TF_i} T_{TF}^S \mathbf{p}_{S_i} \tag{4}$$

where i denotes the index of the pose.

To find T_{TF}^S, an iterative two-step method is proposed, which starts with an initial guess of the matrix. In each iteration, the equations for the planes are found using eigendecomposition, whereafter a set of linear equations is solved for an improved estimate of the desired transformation matrix. The scheme, illustrated in Fig. 2, is iterated until convergence.

A. Finding the calibration planes

Consider initially a set of measurements, $\mathcal{P}_S = [p_1, ..., p_{N_p}]_S$, gathered from a single plane. The normal can be found by Principal Component Analysis (PCA), which amounts to performing an eigendecomposition of the covariance matrix C of the points [8]. The eigenvector corresponding to the smallest eigenvalue of C will be the desired estimate of the plane normal[1]. To this purpose, all points are transformed to a common frame, the robot base frame, using (4) and the current estimate of T_{TF}^S.

To fully specify the plane equation, the center of mass μ of $\mathcal{P}_{RB}$ is calculated. The distance d to the plane is then calculated as the length of the projection of the vector μ onto the plane normal

$$d = \left\| \bar{n}(\bar{n}^\mathsf{T} \mu) \right\| \tag{5}$$

where $\bar{n}$ is a normal with unit length given by PCA. This distance can be encoded into the normal by letting $\|n\| = d$. The normal is then simply found by

$$n = \bar{n}(\bar{n}^\mathsf{T} \mu) \tag{6}$$

This procedure is repeated for all measured calibration planes and results in a set of normals $\mathcal{N}$ that will be used to find the optimal T_{TF}^S.

B. Solving for T_{TF}^S

All measured points should fulfill the equation for the plane they were obtained from. This means that for a single point p

$$\bar{n}^\mathsf{T} p = d \Leftrightarrow n^\mathsf{T} p = \|n\|^2 \tag{7}$$

---

[1]This eigenvalue will correspond to the mean squared distance from the points to the plane.

A measurement point obtained from the sensor in the considered setup should thus fulfill the following set of linear equations

$$\mathbf{p}_{S_i} = \begin{bmatrix} p_{S_i}^\intercal & 1 \end{bmatrix}^\intercal = \begin{bmatrix} x_{S_i} & y_{S_i} & z_{S_i} & 1 \end{bmatrix}^\intercal \quad (8)$$

$$\mathbf{p}_{RB_i} = T_{RB}^{TF_i} T_{TF}^S \mathbf{p}_{S_i} \quad (9)$$

$$n^\intercal p_{RB_i} = \left\| n \right\|^2 \quad (10)$$

where bold-face notation denotes a point expressed in homogeneous coordinates according to (8). Without loss of generality, the points p_S can be assumed to lie on the plane $z_S = 0$. As a result, the third column in T_{TF}^S can not be solved for directly. The constraints on R_{TF}^S to belong to $SO(3)$, will however allow for reconstruction of the third column in R_{TF}^S from the first two columns.

Let $\tilde{T}$ denote the remainder of T_{TF}^S after removing the third column and the last row. Solving the linear equations (9)-(10) for the parameters in $\tilde{T}$ can be expressed as

$$A_i w + q_i = \left\| n_i \right\| \quad \Leftrightarrow \quad A_i w = \left\| n_i \right\| - q_i \quad (11)$$

where $w = \text{vec}(\tilde{T}) \in \mathbb{R}^{9 \times 1}$ consists of the stacked columns of $\tilde{T}$ and

$$A_i = \begin{bmatrix} n_i^\intercal R_{RB}^{TF_i} x_{S_i} & n_i^\intercal R_{RB}^{TF_i} y_{S_i} & n_i^\intercal R_{RB}^{TF_i} \end{bmatrix} \in \mathbb{R}^{1 \times 9} \quad (12)$$

$$q_i = n_i^\intercal p_{RB}^{TF_i} \in \mathbb{R} \quad (13)$$

Since Eqs. (9) and (10) are linear in the parameters, all elements of T_{TF}^S can be extracted into w and A_i can be obtained by performing the matrix multiplications in Eqs. (9) and (10) and identifying terms containing any of the elements of w. Terms with which do not include any parameter to be identified are associated with q_i. The final expressions for A_i and q_i given above can then be obtained by identifying matrix multiplication structures among the elements of A_i and q_i.

Equation (11) does not have a unique solution. A set of at least nine points gathered from at least three planes is required in order to obtain a unique solution to the vector w. This can be obtained by stacking the entries in Eq. (11) according to

$$\mathbf{A}w = \mathbf{Y}, \quad \mathbf{A} = \begin{bmatrix} A_1 \\ A_2 \\ \vdots \\ A_{N_p} \end{bmatrix}, \quad \mathbf{Y} = \begin{bmatrix} \left\| n_1 \right\| - q_1 \\ \left\| n_2 \right\| - q_2 \\ \vdots \\ \left\| n_{N_p} \right\| - q_{N_p} \end{bmatrix} \quad (14)$$

The vector w^* of parameters that minimizes

$$w^* = \arg\min_w \left\| \mathbf{A}w - \mathbf{Y} \right\|_2 \quad (15)$$

can then be obtained from the equation[2] [9], [10]

$$w^* = (\mathbf{A}^\intercal \mathbf{A})^{-1} \mathbf{A}^\intercal \mathbf{Y} \quad (16)$$

Eq. (16) is known as the least-squares solution and the full-rank matrix $(\mathbf{A}^\intercal \mathbf{A})^{-1} \mathbf{A}^\intercal$ is commonly referred to as the pseudo inverse of $\mathbf{A}$. If $\mathbf{A}$ is a square matrix, the

pseudo inverse reduces to the standard matrix inverse. If $\mathbf{A}$ however is a tall matrix, the equation $\mathbf{A}w = \mathbf{Y}$ is over determined and Eq. (16) produces the solution w^* that minimizes Eq. (15).

Since w only contains the first two columns of R_{TF}^S, the third column is formed as

$$R_3 = R_1 \times R_2 \quad (17)$$

where $\times$ denotes the cross product between R_1 and R_2, which produces a vector orthogonal to both R_1 and R_2. The resulting R_{TF}^S will in general not belong to $SO(3)$. The closest valid rotation matrix can be found by Singular Value Decomposition according to [11]

$$R = USV^\intercal \quad (18)$$

$$R^\perp = U \begin{bmatrix} 1 & & \\ & 1 & \\ & & \det(UV^\intercal) \end{bmatrix} V^\intercal \quad (19)$$

or using the matrix square root[3] as [11]

$$R^\perp = R \left(R^\intercal R \right)^{-\frac{1}{2}} \quad (20)$$

The procedure of orthoganalizing R will change the corresponding entries in w^* and the resulting coefficients will no longer solve the problem (15). A second optimization problem can thus be formed to re-estimate the translational part of w, given the orthogonalized rotational part. Let w be decomposed according to

$$w = \begin{bmatrix} \tilde{R}^* & p \end{bmatrix} \quad \tilde{R}^* \in \mathbb{R}^{1 \times 6}, \ p \in \mathbb{R}^{1 \times 3} \quad (21)$$

and denote by $\mathbf{A}_{n:k}$ columns n to k of $\mathbf{A}$. The optimal translational vector, given the orthonormal rotation matrix, is found by solving the following optimization problem

$$\tilde{\mathbf{Y}} = \mathbf{Y} - \mathbf{A}_{1:6} \tilde{R}^* \quad (22)$$

$$p^* = \arg\min_p \left\| \mathbf{A}_{7:9} p - \tilde{\mathbf{Y}} \right\|_2 \quad (23)$$

with the solution

$$p^* = (\mathbf{A}_{7:9}^\intercal \mathbf{A}_{7:9})^{-1} \mathbf{A}_{7:9}^\intercal \tilde{\mathbf{Y}} \quad (24)$$

C. Final Refinement

As noted in [5], solving an optimization problem like (15) is equivalent to minimizing the algebraic distance between the matrix, parameterized by w, and the data. There is no direct minimization of the distances from measurements to planes involved. Given the result from the above procedure as initial guess, any suitable, iterative minimization strategy can be employed to further minimize a cost function on the form

$$J(T_{TF}^S) = \sum_{i=1}^{N_p} (n_i^\intercal p_{RB_i}(T_{TF}^S) - \left\| n_i \right\|)^2 \quad (25)$$

which is the squared distance from the measurement point to the plane. Here, p_{RB_i} is seen as a function of T_{TF}^S according to (9).

---

[2]Commonly solved by `w = A\Y` in Matlab

[3]This method may produce a result with $\det(R)$=-1 if the initial guess is very poor.

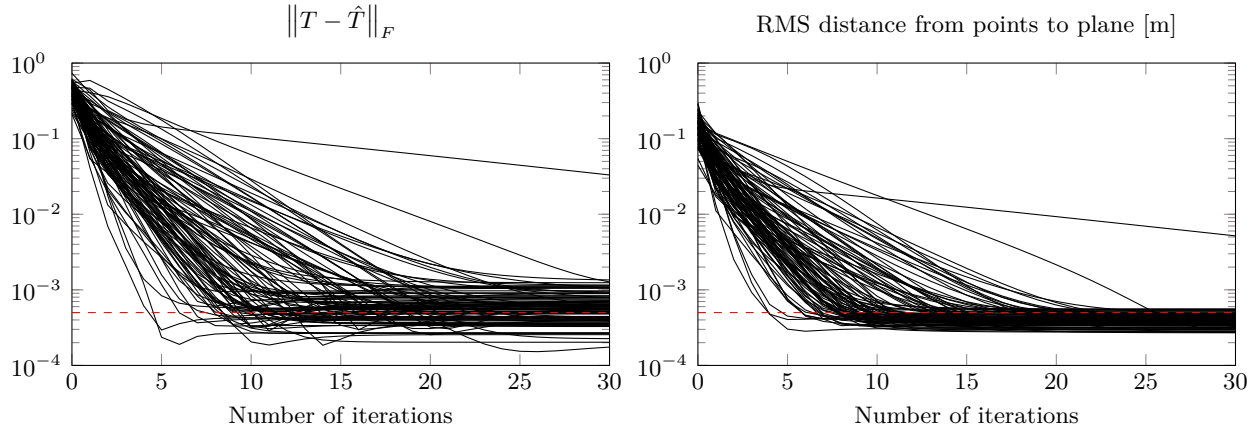$$\left\|T - \hat{T}\right\|_F \qquad \text{RMS distance from points to plane [m]}$$

Fig. 3. Convergence results for simulated data during 100 realizations. 30 poses in total on 3 planes. Measurement noise level $\sigma = 0.5$mm is marked with a red, dashed line. On the left, the Frobenius norm between the true matrix and the estimated, on the right, the RMS distance between measurement points and the estimated plane.

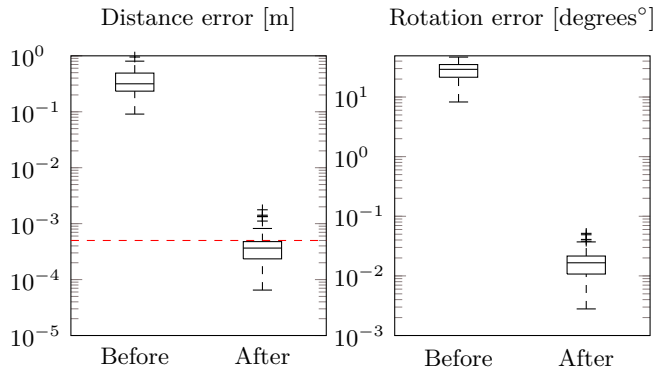Distance error [m]   Rotation error [degrees°]

Fig. 4. Errors in T_{TF}^S before and after calibration for 100 realizations with 30 calibration iterations. 30 poses in total on 3 planes. The measurement noise level $\sigma = 0.5$mm is marked with a dashed line. On the left, the translational error between the true matrix and the estimated, on the right, the rotational error.

TABLE I
DISTRIBUTION OF ERRORS IN INITIAL ESTIMATE OF T_{TF}^S.

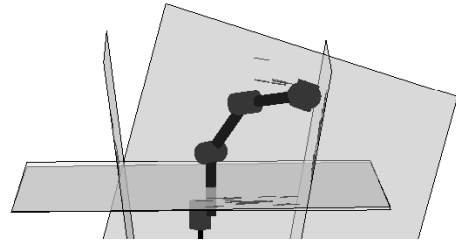|	x, y, z	roll, pitch, yaw
Distribution	$\mathcal{U}(-200\text{mm}, 200\text{mm})$	$\mathcal{U}(-30°, 30°)$

Fig. 5. A visualization of the reconstructed planes used for data collection. The planes were placed so as to be close to orthogonal to each other, surrounding the robot.

IV. RESULTS

The performance of the method was initially studied in simulations, Sec. IV-A, which allows for a comparison between the obtained estimate and the ground truth. The simulation study is followed by experimental verification, Sec. IV-B, using a real laser scanner mounted on the wrist of an industrial manipulator.

A. Simulations

To study the convergence properties of the proposed approach, a simulation study was conducted. A randomly generated T_{TF}^S was used together with measurements from a set of random poses. The initial guess of T_{TF}^S was chosen as the true matrix with an error distributed uniformly according to Table I. The measurements were obtained from three orthogonal planes and corrupted with Gaussian white noise with standard deviation $\sigma = 0.5$mm.

Figure 3 illustrates the convergence for 100 realizations of the described procedure. Most realizations converged to the true matrix within 15 iterations. Analysis shows that careful selection of poses results in faster convergence. The random pose selection strategy employed in the simulation study suffers the risk of co-linearity between measurement poses, which slows down convergence.

Figure 4 illustrates the final results in terms of the accuracy in both the translational and rotational part of the estimate of T_{TF}^S.

B. Experiments

Experimental verification of the proposed method was conducted with a ABB IRB140 robot equipped with a Meta SLS 25 [12] weld seam tracking sensor, see Fig. 1. A whiteboard was placed on different locations surrounding the robot, see Fig. 5, and several measurements of each plane was recorded.

The algorithm was started with the initial guess

$$T_{TF}^S = \begin{bmatrix} 1 & 0 & 0 & 0 \\ 0 & 1 & 0 & 0.15 \\ 0 & 0 & 1 & 0.15 \\ 0 & 0 & 0 & 1 \end{bmatrix} \qquad (26)$$
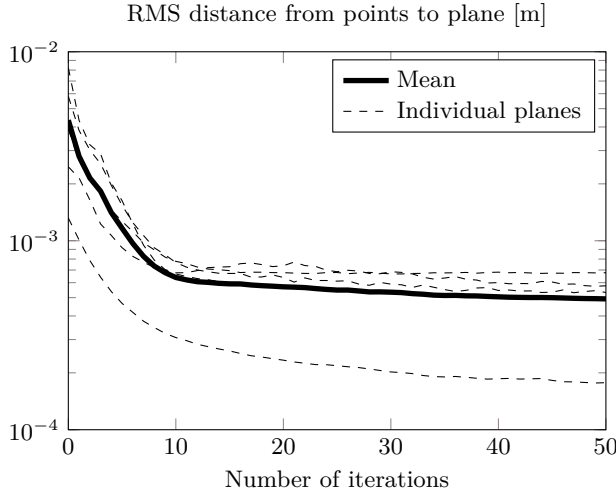
RMS distance from points to plane [m]

Fig. 6. Convergence results for experimental data gathered from 5 planes. The RMS distance between measurement points and the estimated planes are shown together with the mean over all planes.

and returned the final estimate

$$
T_{TF}^{S} = \left[\begin{array}{cccc} 0.9620 & 0.2710 & 0.0010 & 0.0850 \\ -0.2710 & 0.9620 & -0.0240 & 0.1170 \\ -0.0070 & 0.0230 & 1.0000 & 0.1610 \\ 0 & 0 & 0 & 1 \end{array} \right] \quad (27)
$$

The translational part of the initial guess was obtained by estimating the distance from the tool flange to the origin of the laser scanner, whereas the rotation matrix was obtained by estimating the projection of the coordinate axes of the scanner onto the axes of the tool flange[4].

The convergence behavior, illustrated in Fig. 6, is similar to that in the simulation and the final error was on the same level as the noise in the sensor data. A histogram of the final errors is shown in Fig. 7.

V. CONCLUSION

This paper has presented a robust, linear method for the kinematic calibration of a wrist mounted laser sensor. Large uncertainties in the initial estimates are handled and the estimation error converges to below the level of the measurement noise. The calibration routine can be used for any type of laser sensor that measures distances in a plane, as long as the forward kinematics is known, such as when the sensor is mounted on the flange of an industrial robot or on a mobile platform or drone, tracked by an external tracking system.

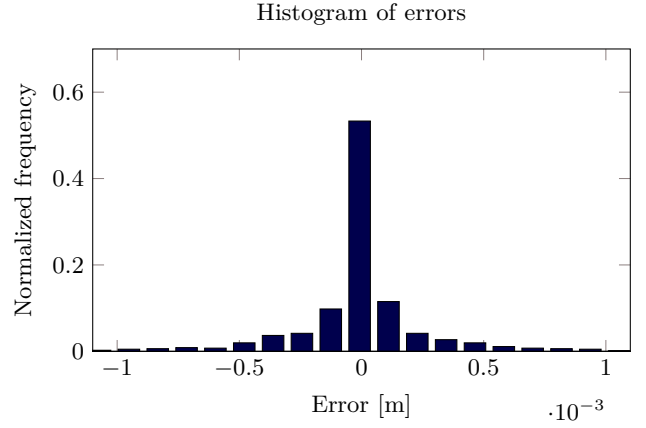[4]The fact that the initial estimate of the rotation matrix was the identity matrix is a coincidence

Histogram of errors

Fig. 7. Histogram of errors $\mathbf{Y} - \mathbf{A}w^*$ for the experimental data.

REFERENCES

[1] K. Daniilidis, "Hand-eye calibration using dual quaternions," *The International Journal of Robotics Research*, vol. 18, no. 3, pp. 286–298, 1999.

[2] R. Y. Tsai and R. K. Lenz, "A new technique for fully autonomous and efficient 3d robotics hand/eye calibration," *Robotics and Automation, IEEE Transactions on*, vol. 5, no. 3, pp. 345–358, 1989.

[3] R. Horaud and F. Dornaika, "Hand-eye calibration," *The International Journal of Robotics Research*, vol. 14, no. 3, pp. 195–210, 1995.

[4] H. Zhuang, S. Motaghedi, and Z. S. Roth, "Robot calibration with planar constraints," in *Robotics and Automation, 1999. Proceedings. 1999 IEEE International Conference on, Detroit, Michigan*, vol. 1, 5 1999, pp. 805–810 vol.1.

[5] Q. Zhang and R. Pless, "Extrinsic calibration of a camera and laser range finder (improves camera calibration)," in *Intelligent Robots and Systems, 2004. (IROS 2004). Proceedings. 2004 IEEE/RSJ International Conference on, Sendai, Japan*, vol. 3, Sept 2004, pp. 2301–2306 vol.3.

[6] M. Ikits and J. Hollerbach, "Kinematic calibration using a plane constraint," in *Robotics and Automation, 1997. Proceedings., 1997 IEEE International Conference on, Pittsburgh*, vol. 4, Apr 1997, pp. 3191–3196 vol.4.

[7] R. S. Hartenberg and J. Denavit, *Kinematic synthesis of linkages*. McGraw-Hill, New York, 1964.

[8] K. Pearson, "On lines and planes of closest fit to systems of points in space," *The London, Edinburgh, and Dublin Philosophical Magazine and Journal of Science*, vol. 2, no. 11, pp. 559–572, 1901.

[9] W. J. Rugh, *Linear system theory*. Prentice-Hall, Englewood Cliffs, 1996.

[10] G. H. Golub and C. F. Van Loan, *Matrix computations*. Johns Hopkins University Press, Baltimore, 2012, vol. 3.

[11] D. W. Eggert, A. Lorusso, and R. B. Fisher, "Estimating 3-d rigid body transformations: a comparison of four major algorithms," *Machine Vision and Applications*, vol. 9, no. 5-6, pp. 272–290, 1997.

[12] Meta Vision Systems. (2014) Meta FSW. [Online]. Available: http://www.meta-mvs.com/fsw